Modeling of Rainfall Erosion

By Pierre Y. Julien[1] and Marcel Frenette[2]

Abstract: A combined stochastic and deterministic method has been developed to evaluate soil erosion from overland flow. The exponential distributions for rainfall duration and intensity are combined with rainfall-runoff relationships for discrete storms. A general equation for sediment discharge is suggested from dimensional analysis with different sets of coefficients representing several existing equations. The expected value of soil erosion during one rainfall event is theoretically derived using hypergeometric series. When applied to the Chaudière watershed near Québec, this equation converges very rapidly, and the first term of the series is recommended. Utilizing sediment-delivery ratios, the sediment yield computed from the total soil erosion is in good agreement with the suspended load measured in the Chaudière River.

Introduction

Soil detachment and transport from upland areas is related to surface runoff, rainfall impact, and vegetation. For bare soils under rainfall, many empirical equations have been proposed to evaluate soil losses from overland flow. However, a general relationship between flow and sediment discharge has not been found yet. The complexity of physical processes between rainfall, overland flow and soil erosion, and also the several man-induced activities, such as land management and agricultural practices, contribute to make the problem of soil erosion a very difficult one to deal with.

Among the first relationships in soil erosion studies, the Musgrave Equation (15) was modified leading to the well-known Universal Soil-Loss Equation (24). Previous investigations by Zingg (29), Meyer and Monke (14), and Young and Mutchler (28) also provided basic understanding of the soil erosion process. For overland flow under simulated rainfall, Kilinc and Richardson (10,11) suggested several sediment transport equations based on regression analysis of experimental data. Li, Shen, and Simons (13) suggested a qualitative equation from analytical considerations. The work of Foster, Smith, Moss, Walker, and others could also be referenced.

Simulation models based on physical processes have been developed more recently by Simons et al. (18,19) and applied to small watersheds. These models use numerical methods to route water and sediment from a watershed for a given rainfall hyetograph. Besides deterministic models, Shen and Li (17) stated that the knowledge for stochastic modeling is rather limited.

The main purpose of this paper is to derive an equation for the expected value of soil erosion and to demonstrate its applicability to wa-

[1]Asst. Prof., Dept. of Civ. Engrg., Colorado State Univ., Fort Collins, Colo.; formerly, Grad. Student at Laval Univ., Québec, Canada.

[2]Prof., Dept. of Civ. Engrg., Laval Univ., Québec, Canada.

Note.—Discussion open until March 1, 1986. To extend the closing date one month, a written request must be filed with the ASCE Manager of Journals. The manuscript for this paper was submitted for review and possible publication on May 8, 1984. This paper is part of the *Journal of Hydraulic Engineering*, Vol. 111, No. 10, October, 1985. ©ASCE, ISSN 0733-9429/85/0010-1344/$01.00. Paper No. 20080.

tershed modeling. First, the fundamental characteristics of rainfall, runoff and sediment discharge are briefly summarized; then, the equation for the expected value of soil erosion by one rainfall event is derived. The last section considers practical applications of the theoretically derived relationship.

Fundamental Characteristics

Rainfall Precipitation.—Point-rainfall precipitation can be described as a random time series of discrete storm events; each event having finite duration and constant intensity. Several stochastic models have been developed by Todorovic, Woolhiser, and Eagleson (3,20,21,22). In these models, the principal variables of rainfall precipitation are: (1) The elapsed time between successive storms; (2) the storm duration; and (3) the storm intensity.

The time of arrival of successive storms has often been described as a Poisson process with intensity λ_0, defined by

$$p(\nu|t) = \frac{(\bar{\nu})^{\nu}}{\nu!} e^{-\bar{\nu}} \qquad (1)$$

with $\bar{\nu} = \lambda_0 t$ (2)

in which $p(\nu|t)$ is the probability to observe ν storms during the time t; $\nu = 0, 1, 2, \ldots$ is the number of storm events; $\bar{\nu}$ is the mean number of storms during the period of time t; and λ_0 is the average arrival rate of storm events during the period t.

The storm duration, t_r, has been found to be distributed exponentially (5). In a general form, if we allow for the variation with time of the duration parameter $\lambda_1(t)$, the probability density function of storm duration $p(t_r)$ is given by

$$p(t_r) = \lambda_1(t)\, e^{-\lambda_1(t)t_r} \qquad (3)$$

If we now consider a period of time that is short enough to assume a constant value of the duration parameter λ_1, we can write in dimensionless form

$$p(\lambda_1 t_r) = e^{-\lambda_1 t_r} \qquad (4)$$

in which $\lambda_1 = \dfrac{1}{\bar{t}_r}$ (5)

in which λ_1 is the reciprocal of the average storm duration, $\bar{t}_r$, during the period, t, considered. Data collected at the Agronomy Station at Laval University from 1966–1970 were available for this study. The observed and fitted distribution functions of rainfall duration $F(t_r)$ corresponding to the integral of Eq. 4 are shown in Fig. 1, for the month of June. Similar graphs were obtained during the rainy season from June–November; these results support those obtained by Eagleson (3) with data from Boston and Santa Paula.

The storm intensity, i, has also been shown to be exponentially distributed with a probability density function, $p(i)$, and an intensity parameter, $\lambda_2(t)$, written as

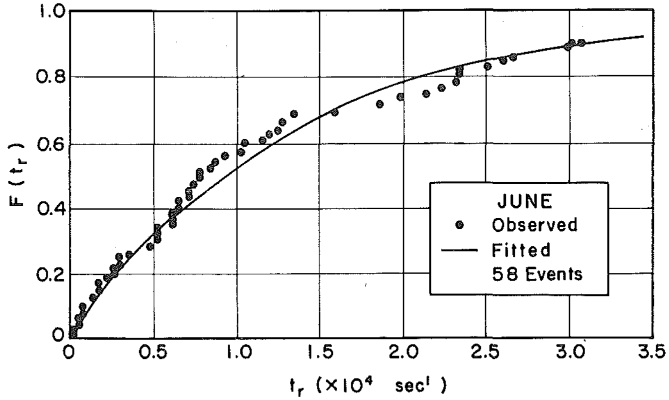

FIG. 1.—Exponential Distribution Function of Rainfall Duration

$$p(i) = \lambda_2(t)e^{-\lambda_2(t)i} \quad (6)$$

which, for short time intervals, reduces to

$$p(\lambda_2 i) = e^{-\lambda_2 i} \quad (7)$$

in which $\lambda_2 = \frac{1}{\bar{i}}$ (8)

and λ_2 is the reciprocal of the average rainstorm intensity, $\bar{i}$. The observed and fitted exponential distribution functions of the rainstorm intensity, $F(i)$, at the same meteorological station are shown in Fig. 2. Similar agreement between observed and fitted exponential distributions was obtained from June to November (8).

In Table 1, the values of the rainfall duration parameters, λ_1, show a gradual decrease through the fall months. Conversely, an increase of the rainfall intensity parameter, λ_2, is observed from September–November. The monthly period selected for evaluating the precipitation parameters,

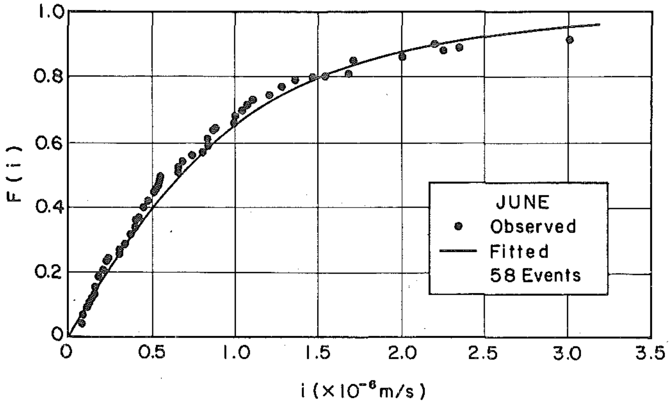

FIG. 2.—Exponential Distribution Function of Rainfall Intensity

TABLE 1.—Monthly Values of Rainfall Duration and Intensity Parameters

Month (1)	$\lambda_1 \times 10^6$, in units per second (2)	$\lambda_2 \times 10^{-5}$, in second per feet (3)
June	42.6	9.15
July	52.4	7.32
August	36.8	9.76
September	36.3	9.15
October	29.4	13.7
November	21.1	15.2

λ_1 and λ_2, seems adequate to allow for the variation of coefficients throughout summer and fall and is also short enough to assume constant values of λ_1 and λ_2 during each month.

Two tests suggested by Yevjevich (27) have been applied to the data to verify the independence between rainfall duration and intensity. The first test is based on the standard deviation of the correlation coefficient and the second uses the standardized variable t. Both tests give identical results and the independence hypothesis has been accepted for all months except October.

Overland Flow and Runoff Hydrographs.—Overland flow refers to the thin surface runoff over upland areas. Sheet runoff over a smooth surface is usually classified as an unsteady nonuniform flow perturbed by raindrop impacts. From experimental data, several authors (2,11,16) have observed overland flow to be laminar.

The two nonlinear partial differential equations derived by Saint-Venant are basically used to solve gradually varied unsteady flow. Considering the relative magnitude of the terms in these equations, the kinematic wave approximation has been most widely recommended (25,26) to define the hydraulics of overland flow.

Laminar flows with raindrop impact can be described by the Darcy-Weisbach equation in which the friction factor, f, is related to: (1) The Reynolds number, R; (2) the friction coefficient, K_o; and (3) the empirical coefficients A and b for raindrop impact. The friction coefficient K includes both effects due to surface roughness and rainfall intensity. The following relationship is generally used

$$f = \frac{K}{\mathsf{R}} = \frac{K_o + Ai^b}{\mathsf{R}} \quad \text{(9)}$$

The values of K_o have been tabulated by Woolhiser (26) for various surface characteristics, and the value $K_o = 24$ is representative of a smooth surface. Various sets of coefficients A and b have been obtained experimentally (4,6,12). For rainfall intensity given in ft/sec, $A = 4.32 \times 10^5$ sec/ft ($A = 1.42 \times 10^6$ s/m for i in m/s); and $b = 1$.

For steady and uniform rainfall intensity over an impervious surface, the time t_e elapsed before the runoff hydrograph reaches an equilibrium state (26) is given by

$$t_e = \left(\frac{K\nu_e L}{8gSi^2}\right)^{1/3} \quad \text{(10)}$$

in which, ν_e is the kinematic viscosity of water; g is the gravitational acceleration; S is the slope; and L is the runoff length. Taking λ (defined as the ratio of the storm duration, t_r to the equilibrium time, t_e), the resulting hydrograph is classified in two distinct types: (1) The complete hydrograph ($\lambda = t_r/t_e > 1$); and (2) the partial equilibrium hydrograph ($\lambda \leqq 1$). These two types of hydrographs are shown in Figs. 3(*a–c*) after the following dimensionless variables for flow discharge ψ and time θ are introduced:

$$\psi = \frac{q}{iL} \quad (11)$$

and $$\theta = \frac{t - t_r}{t_e} \quad (12)$$

in which q is the unit water discharge.

For steady flow conditions in the equilibrium part of the complete hydrograph the average velocity $\bar{u}$, flow depth h, and bottom shear stress τ_o are related to the geometry and to flow characteristics as

$$\bar{u} = \left(\frac{8g}{K\nu_e}\right)^{1/3} S^{1/3} q^{2/3} \quad (13)$$

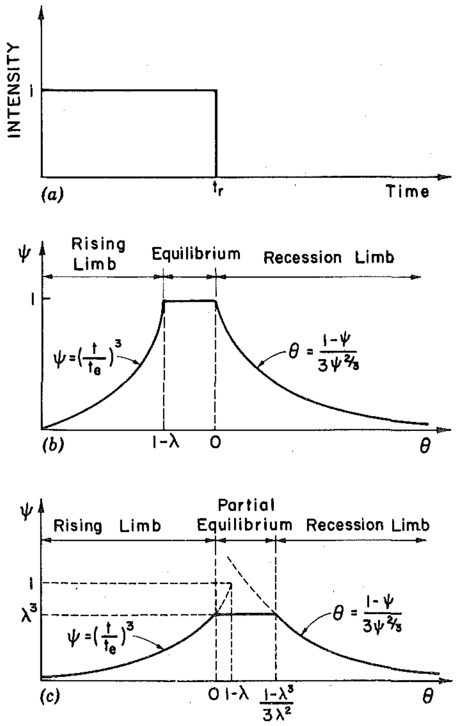

FIG. 3.—Hyetographs and Hydrographs for One Rainfall Event: (*a*) Hyetograph; (*b*) Complete Hydrograph; (*c*) Partial Equilibrium Hydrograph

$$h = \left(\frac{K\nu_e}{8g}\right)^{1/3} S^{-1/3} q^{1/3} \qquad (14)$$

$$\tau_o = \gamma_e \left(\frac{K\nu_e}{8g}\right)^{1/3} S^{2/3} q^{1/3} \qquad (15)$$

in which γ_e is the specific weight of water. It is important to note that soil erosion is often described in terms of these three variables.

Sediment Transport Equations.—Sheet erosion is the result of soil particle detachment and transport from raindrop impact and overland flow. Most eroded soil particles are transported downstream by runoff and the unit sediment discharge is a function of the following variables (8)

$$q_s = f(h, \bar{u}, i, q, L, \tau_o, \tau_c, S, \rho_e, \nu_e, d_s, \rho_s) \qquad (16)$$

in which τ_c is the critical bed shear stress value for the beginning of motion; ρ_e and ρ_s are the density values of water and sediments; and d_s is the size of sediment particles. Elimination of the variables $\bar{u}$ and h is possible from two relationships: the Darcy-Weisbach equation and the continuity equation, $q = \bar{u}h$. The influence of sediment size on sediment transport is considered through the corresponding critical shear stress. Therefore, the sediment size d_s can be eliminated from Eq. 16 using a relationship between τ_c and d_s for laminar flow (23). Eq. 16 thus reduces to

$$f\left(q_s, q, i, L, \rho_e, \nu_e, \frac{\tau_c}{\tau_o}, S, \rho_s\right) = 0 \qquad (17)$$

The following dimensionless groups are obtained from dimensional analysis after L, ρ_s, and q are selected as repeating variables

$$f\left(\frac{q_s}{\rho_s q}, \frac{q}{\nu_e}, \frac{q}{iL}, \frac{\tau_c}{\tau_o}, S, \frac{\rho_s}{\rho_e}\right) = 0 \qquad (18)$$

The first group represents the dimensionless concentration of sediments, the second is the Reynolds number, the third is the flow discharge variable, ψ, defined previously and shown in Figs. 3(*a–c*). The last three groups represent the ratio of critical to bed shear stresses, the slope and the specific gravity of solid particles. After these nondimensional groups are multiplied or divided by other groups to separate the variables q_s, S, q, i, τ_c, and ρ_s, the modified set of dimensionless groups is presented in the following product form:

$$\left(\frac{q_s}{\rho_e \nu_e}\right) = \bar{\alpha} S^{\beta} \left(\frac{q}{\nu_e}\right)^{\gamma} \left(\frac{iL}{\nu_e}\right)^{\delta} \left(1 - \frac{\tau_c}{\tau_o}\right)^{\epsilon} \left(\frac{\rho_s}{\rho_e}\right)^{\eta}; \quad \text{for} \quad \tau_o > \tau_c \qquad (19)$$

In this equation, $\bar{\alpha}$, β, γ, δ, ϵ, and η are experimental coefficients, and the sediment transport equations based on excess tractive force and stream power concepts are best represented by the term $[1 - (\tau_c/\tau_o)]$.

Under dimensional form, this equation is transformed to

$$q_s = \alpha S^{\beta} q^{\gamma} i^{\delta} \left(1 - \frac{\tau_c}{\tau_o}\right)^{\epsilon} \qquad (20)$$

in which, for constant values of the specific gravity, the last group in Eq. 19 is combined with the coefficient α as follows:

$$\alpha = \frac{\bar{\alpha}\rho_e L^\delta}{\nu_e^{\gamma+\delta-1}}\left(\frac{\rho_s}{\rho_e}\right)^\eta \quad (21)$$

Eq. 20 describes a general relationship between sediment discharge, slope, and flow variables. The first three factors (S, q, i) represent the potential erosion (or transport capacity) by overland flow, which is reduced by the last factor describing the soil resistance to erosion. It is also seen that when τ_c is small compared to τ_o, the equation for sediment transport capacity is

$$q_s = \alpha S^\beta q^\gamma i^\delta \quad (22)$$

Quantitative evaluation of the coefficients α, β, γ, δ, and ϵ has been done (8) for several types of equations based on different variables. The equations analyzed are those proposed by Musgrave (15); Li, Shen, and Simons (13); and several regression equations obtained by Kilinc and Richardson (11), including tractive force, stream power, velocity, and discharge equations. When the sediment transport equations in Table 2 are expressed in terms of the variables $\bar{u}$, h, τ_o, and R, the Reynolds number is replaced by $\mathsf{R} = \bar{u}h/\nu_e$, and Eqs. 13–15 are used to transform the variables $\bar{u}$, h, and τ_o into a function of slope and discharge. From the results shown in Table 2, it is found that none of these eight equations is complete since some coefficients are not defined, which reduces the number of variables. The numerical values of the coefficient β vary from 1.21–1.86, and γ varies from 2.03–2.42, except for Eqs. 20*b*–*d* based on tractive force and stream power concepts. The exponents of Eq. 20 are kept variable in the following analysis. Accordingly, evaluation based on each equation in Table 2 will be possible provided the proper set of coefficients is selected.

TABLE 2.—Evaluation of Empirical Coefficients α, β, γ, δ, and ϵ for Several Erosion Equations

Equation number (1)	Equation (2)	Reference (3)	α^a (4)	β (5)	γ (6)	δ (7)	ϵ (8)
20*a*	$q_s = \alpha' S^m L^n i^P$	15	α'	*m*	*n*	*p-n*	—
20*b*	$q_s = \alpha' \int_0^L \tau_o^2\, dx$	13	$3\alpha' \frac{\gamma_e^2}{5}\left(\frac{K\nu_e}{8g}\right)^{2/3}$	1.33	1.67	−1	—
20*c*	$q_s = e^{2.05}(\tau_o - \tau_c)^{2.78}$	10	$e^{2.05}\gamma_e^{2.78}\left(\frac{K\nu_e}{8g}\right)^{0.93}$	1.86	0.93	—	2.78
20*d*	$q_s = e^{0.122}[(\tau_o - \tau_c)\bar{u}]^{1.67}$	10	$e^{0.122}\gamma_e^{1.67}$	1.67	1.67	—	1.67
20*e*	$q_s = e^{-3.17}\bar{u}^{3.625}$	10	$e^{-3.17}\left(\frac{8g}{K\nu_e}\right)^{1.21}$	1.21	2.42	—	—
20*f*	$q_s = e^{1.24}\bar{u}^{4.67}\mathsf{R}^{-0.878}$	10	$e^{1.24}\nu_e^{0.878}\left(\frac{8g}{K\nu_e}\right)^{1.56}$	1.56	2.24	—	—
20*g*	$q_s = e^{-11.6}\mathsf{R}^{2.05}S^{1.46}$	10	$e^{-11.6}\nu_e^{-2.05}$	1.46	2.05	—	—
20*h*	$q_s = e^{11.7}q^{2.035}S^{1.66}$	10	$e^{11.7}$	1.66	2.03	—	—

[a]Sediment discharge in pounds per ft-sec.

Before deriving an expression for the expected soil erosion during a given period of time, the erosion for a single event of given intensity, i, and duration, t_r, must be considered.

Single Event.—Soil erosion by overland flow during a single event, shown in Figs. 4(*a–c*), is obtained by combining Eq. 19 with the flow characteristics corresponding to the runoff hydrograph [Figs. 3(*a–c*)]. In a dimensionless form, the total erosion or mass eroded per unit width, ϕ, is obtained by integrating the sediment discharge, $q_s/\rho_e \nu_e$, over the dimensionless runoff period, $\lambda_1 t$:

$$\phi = \int_0^\infty \frac{q_s}{\rho_e \nu_e} d(\lambda_1 t) = \frac{\lambda_1}{\rho_e \nu_e} \int_0^\infty q_s dt \quad (23)$$

The erosion potential obtained when τ_c reduces to zero in Eq. 20 is

$$\phi = \frac{\lambda_1}{\rho_e \nu_e} \int_0^\infty \alpha S^\beta q^\gamma i^\delta dt \quad (24)$$

For a given constant rainfall intensity i over a plane surface of slope S, Julien (8) integrated Eq. 24 for the complete hydrograph ϕ_c and the partial duration hydrograph ϕ_p

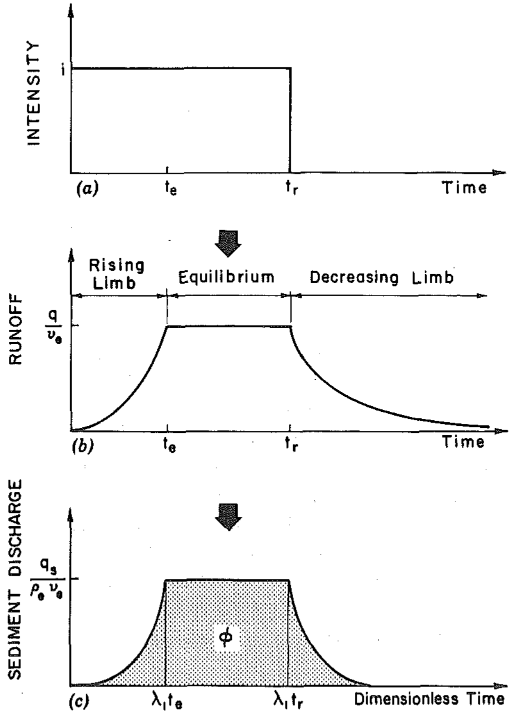

FIG. 4.—Soil Erosion for Single Event: (*a*) Hyetograph; (*b*) Hydrograph; (*c*) Sedimentograph

$$\phi_c = \frac{\lambda_1}{\rho_e \nu_e} \alpha S^{\beta} L^{\gamma} i^{\gamma+\delta} t_r \left[1 - \frac{9}{\lambda}\left(\frac{\gamma^2 - \gamma}{9\gamma^2 - 3\gamma - 2}\right)\right], \quad \lambda > 1 \quad (25)$$

$$\phi_p = \frac{\lambda_1}{\rho_e \nu_e} \alpha S^{\beta} L^{\gamma} i^{\gamma+\delta} t_r \left[\left(\frac{1-\gamma}{3\gamma+1}\right)\lambda^{3\gamma} + \left(\frac{\gamma}{3\gamma-2}\right)\lambda^{3\gamma-3}\right], \quad \lambda < 1 \quad (26)$$

From Table 2, γ normally varies between 1 and 3. When $t_r >> t_e$ (or $\lambda \to \infty$), the term in brackets of Eq. 25 (valid for $\lambda > 1$) reduces to unity. In Eq. 26 (for $\lambda \leqq 1$), the soil erosion ϕ_p remains generally small since for partial duration hydrograph, λ is raised to the power 3γ.

Expected Value of Soil Erosion for One Rainfall Event.—The expected value of soil erosion is determined using the probability density functions of rainfall duration and intensity. These independent exponential distributions were previously described and the expected value of soil erosion by one storm Φ is given by

$$\Phi = \int_0^{\infty}\int_0^{\infty} \phi p(\lambda_1 t_r)\, p(\lambda_2 i)\, d(\lambda_1 t_r) d(\lambda_2 i) \quad (27)$$

From Eqs. 4 and 7, Eq. 27 becomes

$$\Phi = \int_0^{\infty}\int_0^{\infty} \phi e^{-\lambda_1 t_r} e^{-\lambda_2 i}\, d(\lambda_1 t_r)\, d(\lambda_2 i) \quad (28)$$

This integral must be divided in two parts, as indicated by Eqs. 25 and 26, which are valid when $t_r > t_e$ and $t_r \leqq t_e$, respectively. One thus obtains

$$\Phi = \int_0^{\infty}\int_0^{\lambda_1 t_e} \phi_p e^{-\lambda_1 t_r} e^{-\lambda_2 i} d(\lambda_1 t_r)\, d(\lambda_2 i)$$

$$+ \int_0^{\infty}\int_{\lambda_1 t_e}^{\infty} \phi_c e^{-\lambda_1 t_r} e^{-\lambda_2 i}\, d(\lambda_1 t_r)\, d(\lambda_2 i) \quad (29)$$

The boundary value, $\lambda_1 t_e$, is a function of i (Eq. 10), while ϕ_p and ϕ_c are given by Eqs. 25 and 26. The exact analytical solution to Eq. 29 including the variation of the friction factor K with rainfall intensity (Eq. 9) has been obtained using hypergeometric series. The complete solution is written in terms of a series of incomplete gamma functions, which converges very rapidly, and the reader is referred to Julien (8) for the derivation. Experience with field data showed that a constant value of the friction coefficient can be assumed for the evaluation of soil erosion. The representative value of the friction coefficient, K_m, can be computed by substituting $\bar{i}$ for i in Eq. 9 ($K_m = K_o + A\bar{i}^b$). This simplification gives the following approximate solution of Eq. 29.

$$\Phi \cong \frac{\pi_1 \Gamma(\gamma+\delta+1)}{\lambda_1^2 \lambda_2^{\gamma+\delta+1}} - \left[\frac{\pi_1}{\lambda_1}\pi_c\left(\frac{K_m \nu_e L}{8gS}\right)^{1/3} \frac{\Gamma\left(\gamma+\delta+\frac{1}{3}\right)}{\lambda_2^{\gamma+\delta+1/3}}\right] + \ldots \quad (30)$$

in which $\pi_1 = \frac{\lambda_1^2 \lambda_2}{\rho_e \nu_e} \alpha S^{\beta} L^{\gamma}$ . . . . (31)

$$\pi_c = \frac{9\gamma^2 - 9\gamma}{9\gamma^2 - 3\gamma - 2} \quad (32)$$

$$\Gamma(\chi) = \int_0^{\infty} \xi^{\chi-1} e^{-\xi} d\xi: \text{ gamma function} \quad (33)$$

Expected Soil Erosion during Given Period of Time.—The average amount of soil eroded during a given period of time is equal to the product of the expected value of soil erosion for one rainfall event, Φ, and the mean number of events, $\bar{\nu}$, during that period.

$$\bar{\Phi} = \bar{\nu} \Phi \quad (34)$$

Practical Applications

This development has been applied to predict rainfall erosion and sediment yield from the Chaudière Watershed near Québec City, Canada. A detailed description of the methodology including data collection and analysis, discretization of the watershed and computer programs is beyond the scope of this paper. However, the interested reader might refer to previous work (7–9). The writers wish to outline the approach used to cope with practical applications of this theoretical derivation and to provide some of the results obtained.

The significant parameters used to describe the watershed and the monthly rainfall parameters are listed in Table 1. The basin geometry is simplified, and the following parameters are considered: $A_t = 6.27 \times 10^{10}$ ft^2 (5.83×10^9 m^2); $S = 0.0156$; and $L = 300$ ft (91.5 m). The expected value of soil erosion during one rainfall event is computed using numerical integration of the exact formulation (Eq. 29) and the results are compared with the series approximation given by Eq. 30. The exact formulation has been integrated numerically in two different ways: (1) Simple first-order open Newton-Cotes formula (two-dimensional) with 2,500 points; and (2) Gauss quadrature formula (two-dimensional) with 25 points. The results in columns 2 and 3 of Table 3 show that the numerical methods used to solve Eq. 29 give nearly identical results, as one might expect. The results of the series approximation (Eq. 30) are presented in columns 4 and 5 in Table 3 and indicate a very rapid convergence. In this example, the first term of the series can be used to estimate the rate of soil erosion if a 5% error is acceptable. Otherwise, better accuracy is achieved when both terms are considered. Higher order terms in the series were shown to be negligible for the cases investigated. In this example, the expected value of soil erosion after $\bar{\nu}$ storms can be estimated from:

$$\bar{\Phi} = \bar{\nu} \Phi \cong \bar{\nu} \frac{\pi_1 \Gamma(\gamma+\delta+1)}{\lambda_1^2 \lambda_2^{\gamma+\delta+1}} \quad (35)$$

A preliminary sensitivity analysis was conducted to account for water losses due to interception, evapotranspiration, and infiltration. Three cases

TABLE 3.—Expected Value of Soil Erosion by One Rainfall on Chaudière Watershed

	SOIL EROSION IN METRIC TONS			
	Numerical Methods (Eq. 29)		Series Expansion (Eq. 30)	
Month (1)	Newton-Cotes (2)	Gauss (3)	1 term (4)	2 terms (5)
June	48.59	48.15	51.01	48.81
July	62.11	61.54	65.30	62.38
August	49.56	49.12	51.78	49.80
September	57.33	56.32	59.87	57.60
October	30.88	30.60	32.39	31.02
November	34.98	34.67	36.43	35.15

have been studied: (1) No water losses (hyp. A); (2) the water losses reduce the rainfall duration such that the equivalent rainfall duration parameter is $\lambda_{1b} = \lambda_1/C_r$, in which C_r is the runoff coefficient (hyp. B); and (3) the water losses reduce the rainfall intensity and the equivalent rainfall intensity parameter is given by $\lambda_{2c} = \lambda_2/C_r$ (hyp. C). The specific erosion rates based on Eq. 20*b* in Table 2 have been computed as a function of surface slope for these three hypotheses and the results are shown in Fig. 5. These curves represent the potential erosion losses for bare soil. The curve obtained by the empirical Universal Soil-Loss Equation (USLE) under the same conditions (7) is also shown on the same figure. The shape of the quadratic expression for slope in the USLE is very similar to power formulas with an exponent value near 1.7.

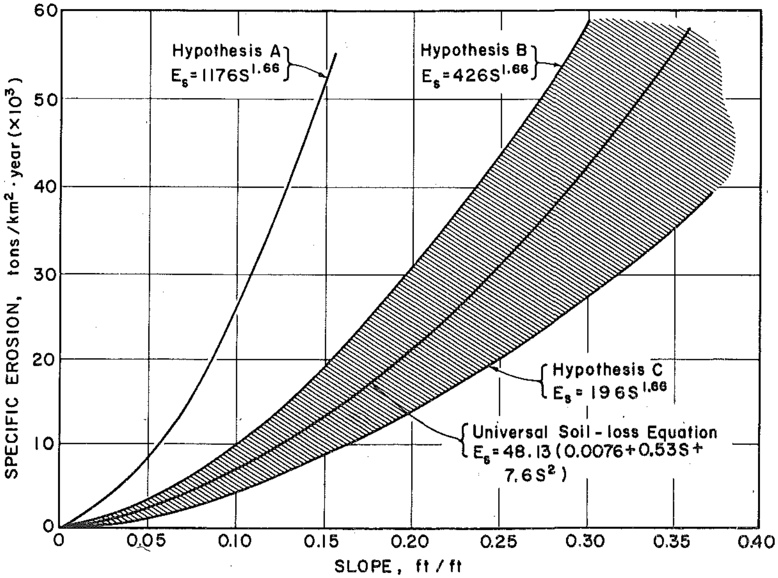

FIG. 5.—Specific Erosion versus Slope on Chaudière Watershed

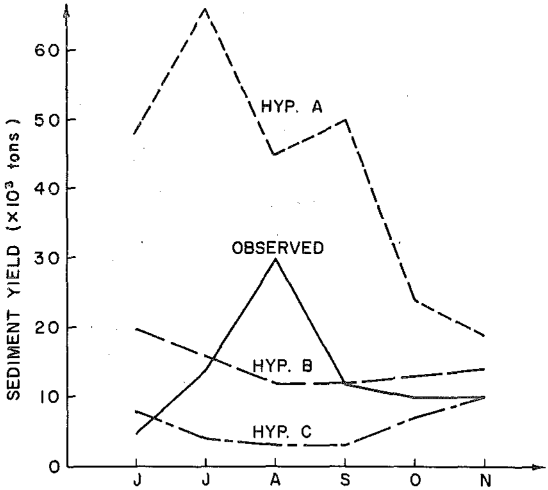

FIG. 6.—Observed and Computed Sediment Yields from Chaudière Watershed

The theoretically derived method has been applied to the Chaudière watershed during the rainfall period (June–November). The cropping management factor of the USLE and the monthly values of the runoff coefficient, C_r, were evaluated to account for vegetation and water losses on the watershed. An average sediment-delivery ratio was estimated from Boyce's data (1,7) to compute monthly sediment yield. These results during the rainfall period are shown in Fig. 6 and compared to the observed suspended load, which is mainly wash load, from 1968–1976 at St-Lambert-de-Lévis near the mouth of the river.

Though the observed values fluctuate, the observed load is in good agreement with the computed sediment yield (hyp. B). The peak in the observed sediment yield for the month of August is related to the occurrence of a severe flood in 1971. The question as to whether hyp. B can be consistently assumed has not yet been fully clarified. However, three other watersheds in Canada were investigated by the writers (9) and the analysis showed that hyp. B gives the best results. In a more detailed analysis of soil erosion and wash load on four northern watersheds (8), this approach to rainfall erosion was extended to soil erosion during snowmelt with excellent results.

Summary and Conclusions

This paper describes a theoretical development in soil erosion modeling based on: (1) The exponential distribution of rainfall duration and intensity; (2) the hydrographs obtained by solving the kinematic wave approximation for the case of a rainfall of constant intensity over an impervious surface; and (3) a general sediment discharge equation for overland flow suggested from dimensional analysis. Two equations for the total soil erosion losses during one rainfall event were derived, respectively, for the complete hydrograph and the partial equilibrium hydrograph. The expected value of the quantity of sediment eroded by a storm has been derived using hypergeometric series and a particular solution (Eq. 30) is determined for the case where the friction factor, K, does not dependent on the rainfall intensity.

It can be concluded that although the general equation (Eq. 29) can be solved analytically in terms of a series of incomplete gamma functions, a very simple first-order approximation (Eq. 35) has been derived from hypergeometric series. This equation has been applied on the Chaudière watershed and gives less than 5% difference with an elaborate numerical evaluation of Eq. 29. Better accuracy can also be obtained by taking the first two terms of the series as shown in Table 3. With the use of the runoff coefficient (hyp. B) and the sediment-delivery ratio, the computed sediment yield compares very well with the observed suspended load in the Chaudière River. The method demonstrated herein has been used to analyze complex watershed configurations and appears to be efficient for studying rainfall erosion and sediment yield from large watersheds.

Acknowledgments

This paper is based on studies carried out at the Department of Civil Engineering at Laval University. The writers wish to thank Dr. P. Todorovic from Ecole Polytechnique, Montréal, for his constructive comments and criticism regarding the rainfall characteristics. The writers are also indebted to Dr. D. B. Simons, G. O. Brown, and J. S. O'Brien from Colorado State University for their kind and helpful suggestions in the revision of this paper.

Appendix I.—References

1. Boyce, R., "Sediment Routing with Sediment-Delivery Ratios. Present and Prospective Technology for Predicting Sediment Yields and Sources," U.S. Department of Agriculture, ARS-S-40, 1975, pp. 61–65.
2. Chen, C. L., "Flow Resistance in Broad Shallow Grassed Channels," *Journal of the Hydraulics Division*, ASCE, Vol. 102, No. HY3, Mar., 1976.
3. Eagleson, P. S., "Climate, Soil and Vegetation, 2. The Distribution of Annual Precipitation Derived from Observed Storm Sequences," *Water Resources Research*, Vol. 14, No. 5, Oct., 1978, pp. 713–721.
4. Fawkes, P. E., "Roughness in a Model of Overland Flow," thesis presented to Colorado State University, at Boulder, Colo., in 1972, in partial fulfillment of the requirements for the degree of Master of Science.
5. Grayman, W. M., and Eagleson, P. S., "Streamflow Record Length for Modelling Catchment Dynamics," *Hydrodynamics Laboratory Report 114*, Department of Civil Engineering, M.I.T., Cambridge, Mass., 1969.
6. Izzard, C. F., "The Surface Profile of Overland Flow," *Transactions of the American Geophysical Union*, Vol. 6, 1944, pp. 959–968.
7. Julien, P., "Erosion de Bassin et Apport Solide en Suspension Dans les Cours d'eau Nordiques," thesis presented to Laval University, at Québec, Canada, in 1979, in partial fulfillment of the requirements for the degree of Master of Science.
8. Julien, P., "Prédiction d'apport Solide Pluvial et Nival Dans les Cours d'eau Nordiques à partir du Ruissellement Superficiel," thesis presented to Laval University, at Quebec, Canada, in 1982, in partial fulfillment of the requirements for the degree of Doctor of Philosophy.
9. Julien, P. Y., and Frenette, M., "A Model for Predicting Suspended Load in

Northern Streams," *Proceedings*, Annual Conference of the Canadian Society for Civil Engineering, CSCE, Halifax, May 23–25, 1984, pp. 565–585.
10. Kilinc, M. Y., "Mechanics of Soil Erosion from Overland Flow Generated by Simulated Rainfall," thesis presented to Colorado State University, at Fort Collins, Colo., in 1972, in partial fulfillment of the requirements for the degree of Doctor of Philosophy.
11. Kilinc, M. Y., and Richardson, E. V., "Mechanics of Soil Erosion from Overland Flow Generated by Simulated Rainfall," Hydrology Paper No. 63, Colorado State University, Fort Collins, Colo., 1973, 54 pp.
12. Li, R. M., "Sheet Flow under Simulated Rainfall," thesis presented to Colorado State University, at Fort Collins, Colo., in 1972, in partial fulfillment of the requirements for the degree of Master of Science.
13. Li, R. M., Shen, H. W., and Simons, D. B., "Mechanics of Soil Erosion by Overland Flow," presented at the 15th Congress, International Association for Hydraulic Research, Istanbul, Turkey, Proc. Paper A54, 1973, pp. 437–446.
14. Meyer, L. D., and Monke, E. J., "Mechanics of Soil Erosion by Rainfall and Overland Flow," *Transactions of ASAE*, Vol. 8, No. 4, 1965, pp. 572–580.
15. Musgrave, G. W., "The Quantitative Evaluation of Factors in Water Erosion: A First Approximation," *Journal of Soil and Water Conservation*, Vol. 2, No. 3, 1947, pp. 133–138.
16. Shen, H. W., and Li, R. M., "Rainfall Effect on Sheet Flow Over Smooth Surface," *Journal of the Hydraulics Division*, ASCE, Vol. 99, No. HY5, Proc. Paper 9733, May, 1973.
17. Shen, H. W., and Li, R. M., "Watershed Sediment Yield Model," *Stochastic Application to Water Resources*, Chapter 21, H. W. Shen, Ed., Water Resource Publication, Fort Collins, Colo., 1976, 68 pp.
18. Simons, D. B., Li, R. M., and Eggert, K. G., "Simple Water Routing and Yield Model Using a Small Programmable Calculator," Colorado State University, *Report for USDA Forest Service*, Rocky Mountain Forest and Range Experiment Station, Flagstaff, Ariz., CER76-77DBS-RML-KGE52, 1977.
19. Simons, D. B., Li, R. M., and Stevens, M. A., "Development of Models for Predicting Water and Sediment Routing and Yield from Storms on Small Watersheds," USDA FOREST Service, Rocky Mountain Forest and Range Experiment Station, Flagstaff, Ariz., CER74-75DBS-RML-MAS24, 1974, 130 pp.
20. Todorovic, P., "A Mathematical Study of Precipitation Phenomena," *Report CER67-68PT65*, Engineering Research Center, Colorado State University, Fort Collins, Colo., 1968.
21. Todorovic, P., and Dawdy, D. R., "Stochastic Point-Rainfall Simulation," *Mathematical Models in Hydrology*, Proceedings of Warsaw Symposium, IAHS-AISH, Publ. No. 100, July, 1971.
22. Todorovic, P., and Woolhiser, D., "Stochastic Model of Daily Rainfall," *Proceedings*, Symposium on Statistical Hydrology, Tucson, Ariz., Misc. Pub. No. 1275, ARS, USDA, June, 1974, pp. 232–246.
23. White, C. M., "The Equilibrium of Grains on the Bed of a Stream," *Proceedings of the Royal Society of London*, Series A, Vol. 174, 1940.
24. Wischmeier, W. H., and Smith, D. D., "Predicting Rainfall Erosion Losses—A Guide to Conservation Planning," *USDA Agriculture Handbook No. 537*, 1978, 58 pp.
25. Wooding, R. A., "A Hydraulic Model for the Catchment Stream Problem, II-Numerical Solutions," *Journal of Hydrology*, Vol. 3, Nos. 3/4, 1965, pp. 268–282.
26. Woolhiser, D. A., "Simulation of Unsteady Overland Flow," *Unsteady Flow in Open Channels*, Chapter 12, K. Mahmood and V. Yevjevich, Eds., Water Resources Publications, Fort Collins, Colo., 1975, pp. 485–508.
27. Yevjevich, V. H., "Statistical and Probability Analysis of Hydrologic Data. Part II. Regression and Correlation Analysis," Section B-II, *Handbook of Applied Hydrology*, V. T. Chow, Ed., McGraw-Hill, New York, N.Y., 1965, 55 pp.

28. Young, R. A., and Mutchler, C. K., "Soil Movement on Irregular Slopes," *Water Resources Research*, Vol. 5, 1969, pp. 184–1089.
29. Zingg, A. W., "Degree and Length of Land Slope as It Affects Soil Loss in Runoff," *Agricultural Engineering*, Vol. 21, No. 2, 1940, pp. 59–64.

Appendix II.—Notation

The following symbols are used in this paper:

A, b = friction coefficients of rainfall intensity;
C_r = runoff coefficient;
d_s = sediment size;
E_s = specific erosion;
$F(i), F(t_r)$ = distribution function of rainfall intensity and duration;
f = Darcy-Weisbach friction factor;
g = gravitational acceleration;
h = flow depth;
i = rainfall intensity;
$\bar{i}$ = average storm intensity;
K = friction coefficient including rainfall effect;
K_o = friction coefficient without rainfall effect;
K_m = representative constant friction coefficient;
L = runoff length;
m, n, p = coefficients of existing sediment discharge equations;
$p(i), p(t_r)$ = probability density function of rainfall intensity and duration;
$p(\nu/t)$ = probability to observe ν storms during the time t;
q = unit water discharge;
q_s^*, q_s = unit sediment discharge by weight and by mass;
R = Reynolds number;
S = land surface slope;
t = time;
t_e = equilibrium time;
t_r = storm duration;
$\bar{t}_r$ = average storm duration;
$\bar{u}$ = depth-integrated flow velocity;
$\alpha, \bar{\alpha}, \beta, \gamma, \delta, \epsilon, \eta$ = coefficients of the general sediment discharge equation;
$\Gamma(\chi)$ = gamma function;
γ_e = specific weight of water and sediment;
θ = dimensionless time variable;
λ = ratio of rainfall duration time to equilibrium time;
λ_0 = average arrival rate of storm events;
λ_1, λ_2 = rainfall duration and intensity parameters;
$\lambda_{1b}, \lambda_{2c}$ = equivalent rainfall duration and intensity parameters;
ν = number of rainfall events;
$\bar{\nu}$ = average number of rainfall events;
ν_e = kinematic viscosity of water;
ξ = dummy variable;
π_1, π_c = group of variables;
ρ_e, ρ_e = density of water and sediments;

τ_o = bed shear stress;

τ_c = critical bed shear stress;

Φ = expected value of soil erosion for one storm;

$\bar{\Phi}$ = expected value of soil erosion during a given period of time;

ϕ = total soil erosion for one storm;

ϕ_c, ϕ_p = total soil erosion during complete and partial equilibrium hydrographs; and

ψ = dimensionless flow discharge.